ELSEVIER

Available online at www.sciencedirect.com

SCIENCE DIRECT®

Thermochimica Acta 426 (2005) 15–21

thermochimica acta

www.elsevier.com/locate/tca

A generalisation of the non-parametric, NPK (SVD) kinetic analysis method
Part 1. Isothermal experiments

G. Roger Heal*

Department of Chemistry, University of Salford, Salford M5 4WT, UK

Received 6 April 2004; received in revised form 26 June 2004; accepted 6 July 2004
Available online 14 August 2004

Abstract

The non-parametric method of kinetic analysis using singular value decomposition of a matrix of data values, as proposed by Nomen and Sempere, is applied to isothermal experiments. It is demonstrated that a correction has to be applied to obtain the value of the pre-exponential constant *A*. The differential analysis method is extended to integral analysis and, when tested using simulated data, shows very accurate retrieval of the starting values of activation energy and pre-exponential constants. A set of data for the decomposition of calcite under vacuum, treated isothermally was taken from the ICTAC study of kinetic methods. The results obtained agree reasonably with those reported from the study.

Keywords: Kinetic analysis; Non-parametric; Singular value decomposition; SVD; Isothermal; Simulated data; Calcite

---

1. Introduction

The use of the non-parametric method of analysis, using singular value decomposition (SVD) of a matrix, has been described by Sempere, Nomen and Serra [1–4] and commented on by Sewry and Brown [5]. The technique was also one of those used in the ICTAC kinetics project [6]. A recent paper by Švadlák et al. [7] has applied the NPK method to the crystallisation of anatase in amorphous TiO_2. The values of activation energy and pre-exponential factors obtained compare favourably with those obtained by conventional analysis methods.

The application of kinetics in thermal studies may be divided up by (a) technique for the experiment and (b) method of analysis. Under (a) the experiment may be carried out under isothermal or non-isothermal conditions. Under (b) the analysis of the data may be by a differential or integral calculation. These experimental techniques and two calculations may thus be combined to give four overall methods. In general terms, the non-isothermal experiment is easier to carry out (with less doubt about the sample temperature), but is the more difficult to analyse by an integral calculation.

The NPK technique, as described in Refs. [1–5], seems to be specifically only applied to one of the four methods described above, namely non-isothermal experiment and differential calculation, but was developed from the analysis of a set of isothermal experiments. There is no reason why the general principles should not be applied to the other two methods. This study is to extend the technique to the all of the methods.

In Part 1 isothermal experiments will be studied and non-isothermal ones in Part 2.

Integral calculations are to be preferred over differential ones, because the data, as obtained from a thermal balance, is integral in nature and requires no processing. The differential calculation requires the determination of the gradients

---

* Present address: 4 Hazelbadge Close, Poynton, Stockport SK12 1HD, UK. Tel.: +44 1625 874850; fax: +44 1625 874850.
E-mail address: roger_heal@yahoo.com (G.R. Heal).

0040-6031/$ – see front matter © 2004 Elsevier B.V. All rights reserved.
doi:10.1016/j.tca.2004.07.004

Table 1
Isothermal experiments

Sample	Starting simulation values		Analysis results		Isoconversional method	
	Input E (kJ/mol)	Input A (s^{-1})	Overall E (kJ/mol)	A (s^{-1})	E (kJ/mol)	A (s^{-1})
Differential analysis						
Simulated A2	130.0	1.0×10^{13}	130.039	1.0119×10^{13}	129.891	0.9728×10^{13}
Calcite in vacuum	–	–	221.9	1.44×10^{11}	211.7	2.98×10^{10}
Integral analysis						
Simulated A2	130.0	1.0×10^{13}	130.0008	1.0005×10^{13}	As above	As above
Calcite in vacuum	–	–	223.6	1.20×10^{11}	As above	As above

Table of activation energies and pre-exponential factors found by analysis using SVD and Isoconversional Arrhenius plot. The results from the simulated data are given to more significant figures than would normally be justified to indicate the precision of the retrieval of the starting figures.

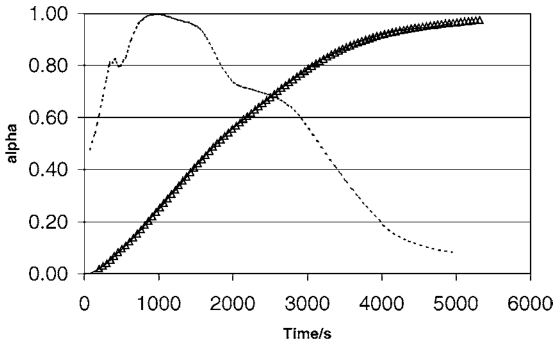

Fig. 1. Isothermal decomposition of calcite at 535 °C (data from CCVISO.TXT [6]): (△) experimental data; (—) fitted line; (- - -) derivative curve.

of the raw data. Since data from a thermal balance is inherently ‘noisy’, the process of differentiation by a curve-fitting routine leads to an exaggeration of the ‘noise’ into random fluctuations and enhanced error in the results [8,9]. This is illustrated in Fig. 1, which is taken from the data used in the ICTAC kinetic study [6], and is for the decomposition of calcite at 535 °C. The experimental or integral data looks reasonably smooth. The differentiated data, shown as a main peak, has developed fluctuations appearing as several superimposed peaks.

The analysis of each method will be studied in turn. Simulated and experimental data was analysed using computer programs developed from these methods. The results for isothermal experiments are shown in Table 1.

2. Isothermal experiments—differential analysis

2.1. Applying SVD

The basic kinetic equation is:

$$\frac{d\alpha}{dt} = kf(\alpha) \tag{1}$$

where α is fraction reacted at time t, k the rate constant and $f(\alpha)$ the kinetic equation obeyed, in its differential form. Many possible equations have been suggested and details of their derivation given [10–12]. If several experiments are carried out at various temperatures, then k may be replaced according to the Arrhenius equation:

$$\frac{d\alpha}{dt} = A\,e^{-E/RT} f(\alpha) \tag{2}$$

where E is activation energy and A the pre-exponential factor.

The purpose of kinetic analysis is to find E, A and which kinetic function $f(\alpha)$ is being obeyed, the so-called kinetic triplet. Eq. (2) may be rewritten as:

$$\frac{d\alpha}{dt} = h(T)f(\alpha) \tag{3}$$

Here, $h(T)$ is a function of temperature and represents $A\,e^{-E/RT}$. The experimental variables are α and T. The principle of the NPK method is to separate the effects of the experimental variables on a total set of data, leading the separation of the functions $h(T)$ and $f(\alpha)$. This should lead to completely independently finding the values of E and A and the function $f(\alpha)$. To carry this out, a matrix **M** has to be filled with values of $d\alpha/dt$. The rows correspond to different values of α and the columns correspond to different temperatures. Each column is thus derived from one experiment. The basis of the NPK method is that the set of $d\alpha/dt$ values in **M** may be separated into two independent functions **f** and **h** without any prior knowledge of their connection to the experimental variables. A consequence of the method is that ln(**h**) plotted against $1/T$ leads to an activation energy and f may be used to find the fit to a kinetic model.

The matrix **M** may be written in matrix notation as:

$$\mathbf{M} = \mathbf{f}\mathbf{h}^{T} \tag{4}$$

where **f** is a vector containing values of $f(\alpha)$ and **h** is a vector containing values of $h(T)$.

The procedure known as SVD (singular value decomposition) takes a matrix such as **M** and decomposes it into three matrices.

$$\mathbf{M} = \mathbf{U}\mathbf{W}\mathbf{V}^{T} \tag{5}$$

If there are n experiments carried out at n temperatures and m values of α chosen, then **M** is (m, n) in size, **U** is (m, n), **V** is

(n, n) and **W** is a vector of size (n). In this application only one element in **W** is significant, $\mathbf{W}(1)$, all other elements being near to zero. This also means that only the first columns of **U** and $\mathbf{V}^{\mathrm{T}}$ are significant and all other elements may be ignored. These sub-sets of **U** and **V** are then vectors and may be called **u** and **v**. Similarly $\mathbf{W}(1)$ may be called **w**. The equation for **M** then becomes:

$$\mathbf{M} = \mathbf{uwv} \tag{6}$$

If **M** is filled with $\mathrm{d}\alpha/\mathrm{d}t$ values at sets of α and temperature, then, after decomposition, **u** contains information on the variation of $f(\alpha)$ with α and **v** contains information on the variation of $A\,\mathrm{e}^{-E/RT}$ with respect to temperature.

The older isoconversional method takes the contents of the matrix **M** one line at a time. Since α is constant across one line, then from the log form of Eq. (2):

$$\ln\left(\frac{\mathrm{d}\alpha}{\mathrm{d}t}\right) = \ln(A) + \ln(f(\alpha)) - \frac{E}{RT} \tag{7}$$

Then a plot of the left-hand side versus $1/T$ gives E from the gradient and $\ln(A) + \ln(f(\alpha))$ from the intercept. The function $f(\alpha)$ has to be known to enable the particular α to be inserted and A to be found.

In the present case, plotting the logarithm of the values of **v** against $1/T$, then using an Arrhenius analysis, allows activation energy E to be found from the gradient.

2.2. Correction of the value of A after finding the function f(α) that fits

The previous papers on this subject [1–5,7] imply that the intercept of this plot is $\ln(A)$, the pre-exponential constant. This is not so. The relative values in **v** are correct, so the correct E is found. However the absolute values in **v** are not correct to yield A. The scale of the quantities in both **u** and **v** are lost in the array decomposition process. A similar decomposition method is described in the book by Malinowski and Howery [13]. The important point that they make on page 47 of their book [13] is that transformation of row and column factors to new reference axes is required to be the next step, before the results can be used. This may be thought of as a rescaling of **U** and **V**. In the present case this is simplified because there is only a single value in $\mathbf{W}(1)$ and the fact that **u** and **v** are vectors, not two-dimensional matrices. If all the values in **v** are multiplied by **w** and by a single value from **u**, then this restores the scale of **v** to that of the original $\mathrm{d}\alpha/\mathrm{d}t$ values. This is just applying Eq. (6) to single values in the vectors. The obvious value of **u** to use is $\mathbf{u}(1)$. This refers to the value corresponding to the first α value, i.e. α_1.

2.2.1. Correction Method 1

The simplest method is to plot the original values of $\ln(\mathbf{v})$, without correction, against $1/T$ and to only correct the resulting intercept as above. The plot yields a provisional intercept I_{p}. The antilog of this is A_{p}. Then this single quantity has to be corrected by multiplying by **w** and $\mathbf{u}(1)$ to restore the scale and to give a corrected intercept A_{c}.

$$A_{\mathrm{c}} = A_{\mathrm{p}}\mathbf{wu}(1) \tag{8}$$

From Eq. (7) the intercept, when $1/T$ equals zero, $\ln(A_{\mathrm{c}})$ is $\ln(A) + \ln(f(\alpha))$, which leads to:

$$A_{\mathrm{c}} = Af(\alpha_1) \tag{9}$$

To be able to find the correct value of A now requires the function $f(\alpha)$ to be known. The finding of the value of A has to be postponed until the correct function is determined.

In the present study, the vector **u** contains the function of α values giving the correct shape when plotted against α; but the scale is wrong. Rescaling to match the various theoretical curves, $f_{\mathrm{t}}(\alpha)$, for each of the possible kinetic equations allows a match to be made and a choice of equation. The value of $f(\alpha)$ was determined at the mid-point in the experimental data in **u**. Also the mid-point value of $f_{\mathrm{t}}(\alpha)$, from the theoretical equations was found. The ratio of the mid-point in $f(\alpha)$ to the mid-point in $f_{\mathrm{t}}(\alpha)$ was called correction factor F. The theoretical data was multiplied by F to make the curves match perfectly at that point. The rescaling was carried out in this way so that, on stepping through the set of theoretical equations, the experimental points remained at the same place on successive graphs. An alternative test is to plot **u** ($f(\alpha)$ experimental) values against $f_{\mathrm{t}}(\alpha)$ (values for the theoretical equations) which should form a straight line if the experimental and theoretical equations match. These tests were then repeated for each theoretical equation in turn. A set of 28 kinetic equations to be used was taken from reference [12].

2.2.2. Correction Method 2

In theory, the correction factor F also gives the corrected pre-exponential constant. Instead of correcting $f_{\mathrm{t}}(\alpha)$ to match $f(\alpha)$, the reverse could be carried out, i.e. dividing $f(\alpha)$ values by F should give values that match $f_{\mathrm{t}}(\alpha)$. The new quantity $f(\alpha)/F$ gives rescaled values of **u**. To preserve Eq. (6) then the **v** values have also to be multiplied by F, i.e. $\mathbf{M} = (\mathbf{u}/F)\mathbf{w}(\mathbf{v}F)$. Combining Eqs. (8) and (9) produces $A = A_{\mathrm{p}}\mathbf{wu}(1)/f(\alpha_1)$. The factor F then has the same value as $\mathbf{wu}(1)/f(\alpha_1)$. Thus multiplying the initial value of pre-exponential factor by F gives the true value of A, i.e. $A = A_{\mathrm{p}}F$. This works very well for the simulated data, where the experimental and theoretical plots match exactly.

To summarise, Method 1 derives a correction factor for A from **w** and $\mathbf{u}(1)$, while Method 2 derives the correction from the matching of experimental and theoretical $f(\alpha)$ curves. For experimental data, such as in Fig. 7, accurate matching is too difficult, so F would only be very approximate. In this case the use of Correction Method 1 using Eqs. (8) and (9) is preferred.

2.3. Interpolation along the data curves

The data requires differentiation and several methods were tried and tested to see if the corresponding smoothing of the original data produces results that compare correctly with the original data. In some cases a cubic equation fit, changing to a quadratic fit near the top end, was good enough. This worked well enough for simulated data, but experimental data was better treated by a polynomial fit, where the degree of the equation and the number of points used, above and below the fitted position, could be varied.

The treatment requires that $\mathrm{d}\alpha/\mathrm{d}t$ is determined at corresponding values of α for all the data curves. For this purpose the gradients were calculated at standard values of α from 0.01 to 0.99 in steps of 0.01.

3. Isothermal experiments—integral analysis

3.1. Applying SVD

If Eq. (1) is integrated at constant temperature this gives:

$$\int \frac{\mathrm{d}\alpha}{f(\alpha)} = \int k\,\mathrm{d}t \quad \text{or} \quad g(\alpha) = kt \tag{10}$$

Varying temperature for a set of curves gives:

$$g(\alpha) = A\,\mathrm{e}^{-E/RT}t \tag{11}$$

This may be transposed to:

$$t = g(\alpha)\frac{1}{A\,\mathrm{e}^{-E/RT}} \tag{12}$$

In this case it is time **t** that corresponds to **M** in Eq. (6) and is a function of α and T. $g(\alpha)$ corresponds to **u** and $1/(A\,\mathrm{e}^{-E/RT})$ to **v**. This **t** then represents a matrix of values which may also be analysed by SVD. The method is still an NPK study because the matrix of **t** values may be decomposed into **u** and **v** without prior knowledge of the functions that they represent. Interpolation has to be carried out along each set of experimental curves, at one temperature, to find the **t** values at standard α values. Again α from 0.01 to 0.99 in steps of 0.01 was used. A matrix of **t** values was made up and decomposed by SVD. This time the log of the reciprocal of the **v** vector values was plotted against $1/T$, as the Arrhenius plot, to obtain E. The **u** vector was matched this time against rescaled, theoretical integral functions $g_t(\alpha)$, for all of the equations tested. The intercept of the **v** plot again apparently gave A, but required correction as explained in Section 2.2.1. Eq. (8) was used as before but, because the reciprocal of **v** had to be plotted, Eq. (9) became $A_c = A/g(\alpha_1)$, so $A = A_p\mathbf{wu}(1)\cdot g(\alpha_1)$. Also, if the value of correction factor F is used as in Section 2.2.2, instead of Eqs. (8) and (9), then it has to divide the initial value of the pre-exponential constant to obtain the true value of A, i.e. $A = A_p/F$.

4. Testing with simulated data

A computer program was written in Fortran 77 to carry out the analysis. This included a standard SVD algorithm taken from the Netlib repository [14]. Also used, was a generator program to simulate isothermal data.

The floating-point variables were declared as double precision to increase precision. The α values transferred from the simulation generator program to the analysis program, via data files, were given to 20 significant figures. This is, of course, far more precise than any thermal balance can produce, but was thought necessary to be able to prove how accurately the starting values of E and A were recovered.

4.1. Isothermal data by a differential analysis

Data for several of the kinetic equations mentioned in Refs. [10–12] was created and tested using the above theory. The activation energy E used in the simulation in most cases was 130 kJ/mol and the value of A was $10^{13}\,\mathrm{s}^{-1}$.

An example given is for equation A2 (mechanism 14 from Ref. [12]), which is, in differential form:

$$\frac{\mathrm{d}\alpha}{\mathrm{d}t} = A\,\mathrm{e}^{-E/RT}(1-\alpha)[-\ln(1-\alpha)]^{1/2} \tag{13}$$

The temperatures used were 476–481 K in steps of 1 K. Analysis was carried out as explained in Section 2. The plot of ln(**v**) versus $1/T$ is shown in Fig. 2. Minus the gradient of the line, times R, gave the value of E the activation energy. The values in the first column of **u** were plotted against α in Fig. 3, together with each rescaled theoretical equation in turn. The fit for Eq. (13) should, of course, be perfect, as is shown. A plot was also made of $f(\alpha)$, for the experimental data (the **u** values) against $f_t(\alpha)$, for each theoretical equation in turn. The result was again a perfect correlation for Eq. (13), as shown in Fig. 4. Once the best-fit equation was decided to be (13), the value $f(\alpha_1)$ for the first point, i.e. $f(0.01)$, could then be found. The initial intercept gave a value of A_p as $6.3182 \times 10^{13}\,\mathrm{s}^{-1}$. When treated according to Eqs. (8) and (9), this gave a value of A of $1.0119 \times 10^{13}\,\mathrm{s}^{-1}$. The results in Table 1 are in good agreement with the starting values for the simulation.

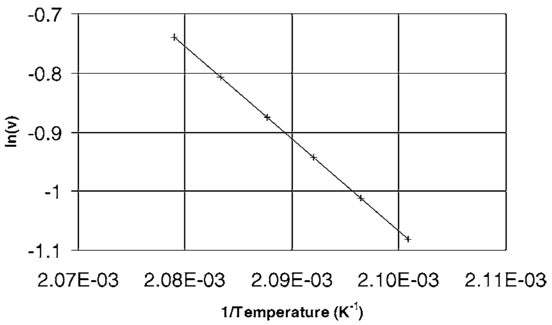

Fig. 2. Differential analysis of isothermal data. Arrhenius plot of ln(**v**), i.e. ln(rate) vs. $1/T$ for simulated isothermal data for mechanism A2, i.e. Eq. (13).

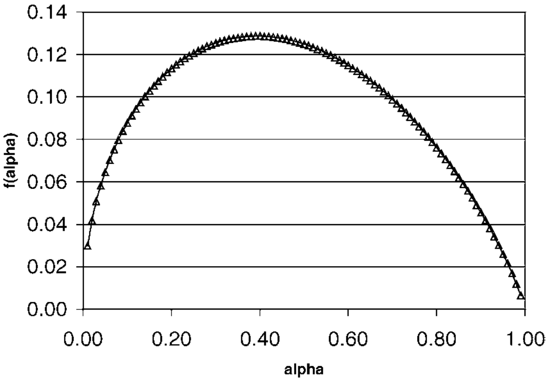

Fig. 3. Differential analysis of isothermal data ($f(\alpha)$ vs. α). The data is simulated from mechanism A2, i.e. Eq. (13). The theoretical $f(\alpha)$ are also for mechanism A2, i.e. Eq. (13). The experimental and theoretical data are superimposed: (△) experimental $f(\alpha)$; (—) theoretical $f(\alpha)$ (rescaled values).

Under some circumstance the corrections implied in Eqs. (8) and (9) may not be required. Some kinetic equations that are used for simulation, or happen to fit experimental data, have finite values for gradient at $\alpha = 0$ which also happen to equal unity. It may then be that data is included for $\alpha = 0$ in the matrix, i.e. $\alpha_1 = 0$. Under these circumstances the value of **u**(1) would be 1 and $f(\alpha_1) = 1$, so the intercept from the Arrhenius plot gives the value of A directly. Examples of this are for equations such as:

$$\frac{\mathrm{d}\alpha}{\mathrm{d}t} = k(1-\alpha)^n, \quad n = 1, 2, \frac{1}{2}, \frac{2}{3}, \frac{1}{3}, \frac{4}{3} \tag{14}$$

However, other equations like:

$$\frac{\mathrm{d}\alpha}{\mathrm{d}t} = k\alpha^m, \quad m = 1, \frac{1}{2}, \frac{2}{3}, \frac{3}{4} \tag{15}$$

Also all of the Avrami–Erofeev types and most diffusion types have gradients of zero at $\alpha = 0$. The SVD algorithm fails if a row of values of gradients are all zero. Also, a value of $f(\alpha_1)$ of zero in Eq. (9) would be meaningless. Data was also simulated for equation F1, i.e. $\mathrm{d}\alpha/\mathrm{d}t = k(1-\alpha)$. The interpolation for α values was continued down to $\alpha = 0.0$. The value of E obtained was 129.989 kJ/mol and the value of A obtained was 0.9973×10^{13}, directly from the intercept, with no use of Eqs. (8) and (9), or multiplication of the **v** values by **u**(1). However, multiplication by **w** was still carried out. In practice, since the kinetic function would not be known at the start, it is not possible to use this approach for some equations. Even if the equation that fits is suspected beforehand, it would not be good practice to use the finite gradient at $\alpha = 0$ because, at zero time in an isothermal experiment, the sample cannot have reached the correct isothermal decomposition temperature. Indeed it might not be possible to produce accurate data at a point as low as $\alpha = 0.01$, and calculation should be postponed until the temperature has settled to a constant value. The whole calculation should then be started at a higher α value.

4.2. Isothermal data by an integral analysis

The method was applied to the same simulated data as above generated from Eq. (13). The Arrhenius plot produced was similar to Fig. 2 for the differential treatment, but with a different ordinate scale. This also illustrates the fact that these plots do not directly give the value of A from the intercept. The method of fitting the correct equation was to plot the integral version of the kinetic equation, $g(\alpha)$ versus α, attempting to find a coincidence for a theoretical equation with the experimental result, as shown in Fig. 5. Like the differential analysis, a perfect fit was found for Eq. (13). The initial value for A_p was $3.857 \times 10^{14}\ \mathrm{s}^{-1}$, very different from that for the differential analysis. Calculating the value A from Eqs. (8) and (9) gave $1.0005 \times 10^{13}\ \mathrm{s}^{-1}$. A rather large number of significant figures have been quoted to illustrate the precision of the method and it proves to be more precise than the differential method above.

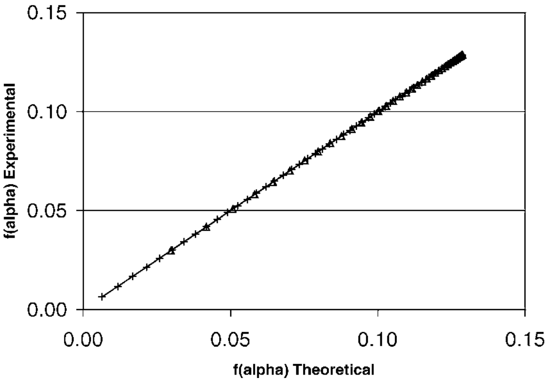

Fig. 4. Differential analysis of isothermal data. Experimental $f(\alpha)$ vs. theoretical $f(\alpha)$ (rescaled values). The data is simulated from mechanism A2, i.e. Eq. (13). The theoretical $f(\alpha)$ are also mechanism A2, i.e. Eq. (13): (△) points where $f(\alpha)$ is rising; (+) points where $f(\alpha)$ is falling; (—) best fit line to all the points.

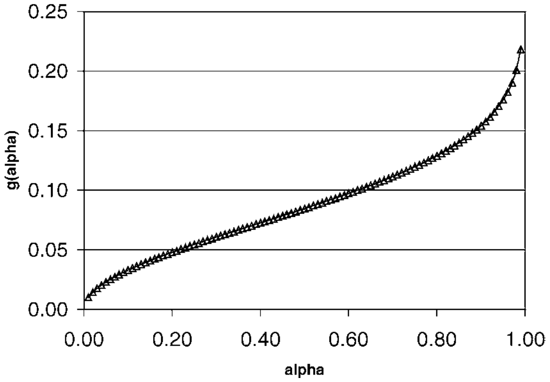

Fig. 5. Integral analysis of isothermal data ($g(\alpha)$ vs. α). The data is simulated from mechanism A2, i.e. Eq. (13). The theoretical $g(\alpha)$ are also for mechanism A2, i.e. Eq. (13). The experimental and theoretical data are superimposed: (△) experimental $g(\alpha)$; (—) theoretical $g(\alpha)$ (rescaled values).

5. Testing with experimental data

5.1. Isothermal data by a differential analysis

The analysis described was applied to the set of data from the ICTAC kinetics project [6] for the isothermal decomposition of calcite under vacuum (CCVISO.TXT in the nomenclature used in the paper). This was chosen because of the amount of comment on the analysis of this data that has been published [6,15–18]. The experiments were conducted at 550, 540, 535, 530, 520 and 515 °C. One set of data is shown in Fig. 1. The differential plots for the other temperatures were like Fig. 1, showing similar fluctuations. The Arrhenius plot in Fig. 6 was reasonably straight. Attempts to match the $f(\alpha)$ experimental values against theoretical showed that the fluctuation produced in the differentiation had been transmitted to the values in matrix **u**, so appear in Figs. 7 and 8. The choice of the correct equation was difficult but, from the appearance of Fig. 7, it looks as if kinetic equation A5 (mechanism 17 from Ref. [12]), Eq. (16) would be the nearest fit.

$$\frac{d\alpha}{dt} = A\,e^{-E/RT}(1-\alpha)[-\ln(1-\alpha)]^{1/3} \qquad (16)$$

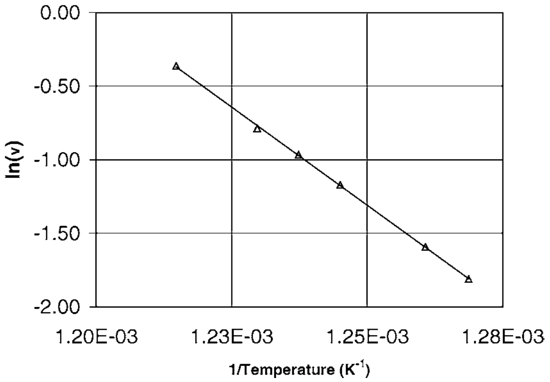

Fig. 6. Differential analysis of isothermal data. Arrhenius plot of ln(**v**), i.e. ln(rate) vs. $1/T$ for isothermal data for calcite decomposition under vacuum (CCVISO.TXT [6]).

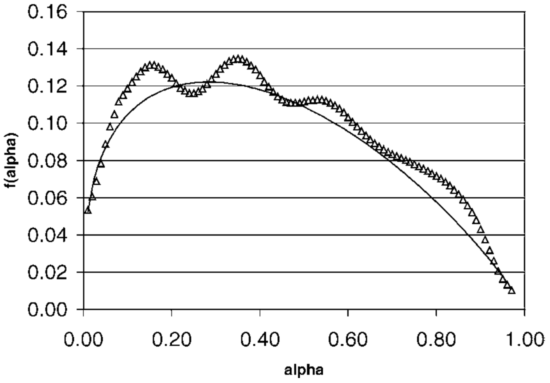

Fig. 7. Differential analysis of isothermal data. $f(\alpha)$ vs. α for isothermal data for calcite decomposition under vacuum (CCVISO.TXT [6]). The theoretical $f(\alpha)$ are for mechanism A5 or Eq. (16). The experimental and theoretical data are superimposed: (△) experimental $f(\alpha)$; (—) theoretical $f(\alpha)$ (rescaled values).

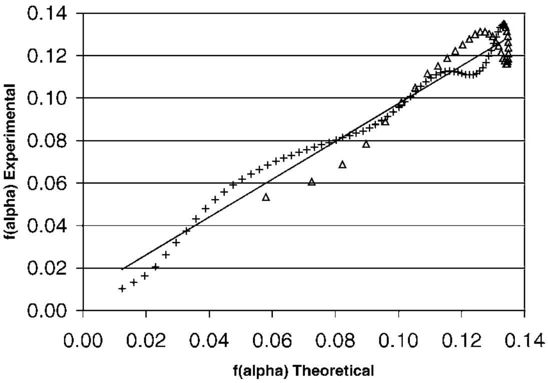

Fig. 8. Differential analysis of isothermal data. Experimental $f(\alpha)$ vs. theoretical $f(\alpha)$ values for isothermal data for calcite under vacuum (CCVISO.TXT [6]). The theoretical $f(\alpha)$ are for mechanism A5, i.e. Eq. (16): (△) points where $f(\alpha)$ is rising; (+) points where $f(\alpha)$ is falling; (—) best fit line to all the points.

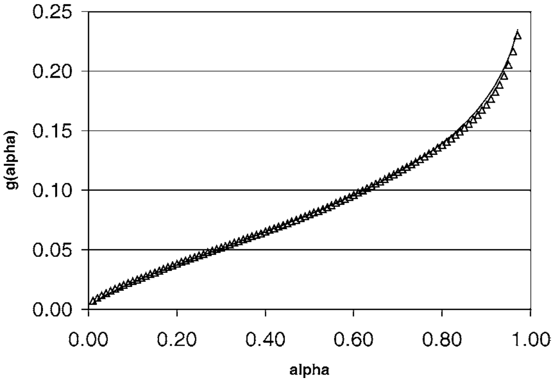

Fig. 9. Integral analysis of isothermal data. $g(\alpha)$ vs. α values for isothermal data for calcite under vacuum (CCVISO.TXT [6]). The theoretical $g(\alpha)$ are for mechanism A5 or Eq. (16). The experimental and theoretical data are superimposed: (△) experimental $g(\alpha)$; (—) theoretical $g(\alpha)$ (rescaled values).

5.2. Isothermal data by an integral analysis

Extending integral analysis to the CCVISO.TXT data produced an activation energy and a final value for A close to those by differential analysis. The test for the equation fitting gave Fig. 9. Equation A5 as still the best fit, except at higher α. Comparing Fig. 9 to Fig. 7, all trace of the fluctuation shown in the differential analysis has gone.

6. Conclusions

Table 1 shows that, for simulated data, the methods described retrieve the values of E and A with reasonable precision. The precision is greater for integral analysis as compared to differential analysis. Identification of the correct kinetic equation was clear for this simulated data. For the experimental data, the differential method of analysis shows a fluctuation in the value of activation energy caused by the process of differentiation of the original data. The theoretical fitted much more clearly if integral analysis was used.

References

[1] J. Sempere, R. Nomen, R. Serra, Thermochim. Acta 316 (1998) 37–45.
[2] J. Sempere, R. Nomen, R. Serra, J. Therm. Anal. Calorim. 52 (1998) 933–943.
[3] J. Sempere, R. Nomen, R. Serra, J. Therm. Anal. Calorim. 56 (1999) 843–849.
[4] J. Sempere, R. Nomen, R. Serra, J. Soravilla, Thermochim. Acta 388 (2002) 407–414.
[5] J.D. Sewry, M.E. Brown, Thermochim. Acta 390 (2002) 217–225.
[6] M.E. Brown, M. Maciejewski, S. Vyasovkin, R. Nomen, J. Sempere, A. Burnham, J. Opfermann, R. Strey, H.L. Anderson, A. Kremmler, R. Keuleers, J. Janssens, H.O. Desseyn, C.-R. Li, T.B. Tang, B. Roduit, J. Malek, T. Mitsuhashi, Thermochim. Acta 355 (2000) 125–143.
[7] D. Švadlák, J. Shánělová, J. Málek, L.A. Pérez-Maqueda, J.M. Criado, T. Mitsuhashi, Thermochim. Acta 414 (2004) 137–143.
[8] J.H. Flynn, L.A. Wall, J. Res. Nat. Bur. Stand., A. Phys. Chem. 70A (6) (1966) 506.
[9] G.R. Heal, in: P.J. Haines (Ed.), Principles of Thermal Analysis, Royal Society of Chemistry Paperbacks, 2002, p. 29.
[10] J. Sestak, V. Satava, W.W. Wendlandt, Thermochim. Acta 7 (1973) 333.
[11] M.E. Brown, D. Dollimore, A.K Galwey, in: C.H. Bamford, C.F.H. Tipper (Eds.), Comprehensive Chemical Kinetics, vol. 22, Elsevier, Amsterdam, 1980, p. 340.
[12] C.F. Dickinson, G.R. Heal, Thermochim. Acta 340/341 (1999) 89–103;
C.F. Dickinson, PhD Thesis, Salford University, 2000, p. 31.
[13] E.D. Malinowsky, D.G. Howery, Factor Analysis in Chemistry, Wiley, New York, 1980.
[14] Netlib Repository, see: http://netlib.ccp14.ac.uk/eispack/svd.f.
[15] M. Maciejewski, Thermochim. Acta 355 (2000) 145–154.
[16] A.K. Burnham, Thermochim. Acta 355 (2000) 165–170.
[17] B. Roduit, Thermochim. Acta 355 (2000) 171–180.
[18] S. Vyasovkin, Thermochim. Acta 355 (2000) 155–163.